Molecular Therapy
Nucleic Acids
Original Article

A Novel Pak1/ATF2/miR-132 Signaling Axis Is Involved in the Hematogenous Metastasis of Gastric Cancer Cells

Funan Liu,[1,2,3] Zhenguo Cheng,[1,3] Xiaodong Li,[1] Yanshu Li,[1] Hongyan Zhang,[1] Jiabin Li,[1] Furong Liu,[1] Huimian Xu,[2] and Feng Li[1]

[1]Department of Cell Biology, Key Laboratory of Cell Biology, Ministry of Public Health and Key Laboratory of Medical Cell Biology, Ministry of Education, China Medical University, Shenyang 110122, China; [2]Department of Surgical Oncology and General Surgery, The First Affiliated Hospital of China Medical University, Shenyang 110122, China

We, along with others, have shown previously that P21-activated kinase 1 (Pak1) plays a pivotal role in gastric cancer progression and metastasis. However, whether Pak1 controls gastric cancer metastasis by regulating microRNAs (miRNAs) has never been explored. Here, we report a novel mechanism of Pak1 in tumor metastasis. A detailed examination revealed that Pak1 interacts with and phosphorylates the serine 62 residue of ATF2 and then blocks its translocation into the nucleus. We also confirmed that ATF2 binds to the promoter of miR-132 and tightly regulates its transcription, thus explaining the regulatory mechanism of miR-132 by Pak1. miR-132 also significantly reduced cell adhesion, migration, and invasion of gastric cancer cells in vitro and significantly prevented tumor metastasis in vivo. miR-132 specifically inhibited hematogenous metastasis, but not lymph node or implantation metastases. In order to further delineate the effects of the Pak1/ATF2/miR-132 cascade on gastric cancer progression, we identified several targets of miR-132 using a bioinformatics TargetScan algorithm. Notably, miR-132 reduced the expression of CD44 and fibronectin1 (FN1), and such inhibition enabled lymphocytes to home in on gastric cancer cells and induce tumor apoptosis. Taken together, our studies establish a novel cell-signaling pathway and open new possibilities for therapeutic intervention of gastric cancer.

INTRODUCTION

P21-activated kinase 1 (Pak1), a serine/threonine kinase, plays critical roles in cytoskeletal remodeling, cell motility, apoptosis, and transformation,[1,2] and it affects many distinct signal transduction pathways. Pak1 has been strongly implicated in several human cancers. It confers invasiveness to breast cancer cells in response to heregulin-beta1-mediated ErbB2 stimulation,[3] and it is overexpressed in breast tumors.[4] Pak family members, in general, have been shown to be involved in several oncogenic processes.[5–7] PAKs play pivotal roles in many cellular processes that confer cancer phenotype, including invasion, metastasis, anti-apoptosis, drug resistance, angiogenesis, epithelial-to-mesenchymal transition (EMT), DNA-damage repair, modulation of gene expression, and changes in progression of mitosis and cell cycle.[8] Pak1 facilitates enhanced cell survival, including that of oncogenic cells, by preventing apoptosis through at least three different pathways that involve forkhead box O1 (FOXO1), B cell chronic lymphocytic leukemia (CLL)/lymphoma 2 (Bcl-2), or DLC1.[9,10] Pak1 also regulates the activity of Raf and Aurora kinases and affects cellular proliferation.[11] Overexpression of Pak1 is involved in the regulation of actin assembly and disassembly through phosphorylation of LIM kinase and cytoskeletal-associated proteins such as filamin A, paxillin, caldesmon, cortactin, and Arp2/3.[12]

Gastric cancer is the fourth most common cancer in the world and has the second highest mortality rate.[13] Although recent advances in the treatment of gastric cancer have improved the clinical outcomes, the 5-year survival rate is still ~30%, and the prognosis of remains very poor.[14] Tumor invasion and metastasis are the major impediments to a clear prognosis. When diagnosed, 20% to 30% of the patients already have distant organ metastasis, most commonly to the liver and lung by hematogenous metastasis.[15] Our previous studies and those of others have shown that Pak1 signaling has a profound effect on gastric cancer.[2]

MicroRNAs (miRNAs) are non-coding small RNA molecules that regulate gene expression at the post-transcriptional level by binding to the 3′ UTR of their target mRNAs and repress protein production by destabilizing mRNA and silencing translation.[16] Many miRNAs have been shown to play crucial roles at a number of steps that confer tumor metastasis, including EMT, anoikis, angiogenesis, invasion, and migration.[17] Although our previous data and other studies have confirmed that some miRNAs can inhibit tumor proliferation

Received 19 January 2017; accepted 5 July 2017;
http://dx.doi.org/10.1016/j.omtn.2017.07.005.

[3]These authors contributed equally to this work.

Correspondence: Feng Li, Department of Cell Biology, Key Laboratory of Cell Biology, Ministry of Public Health and Key Laboratory of Medical Cell Biology, Ministry of Education, China Medical University, No. 77 Puhe Road, Shenyang North New Area, Shenyang 110122, China.
E-mail: lifeng@cmu.edu.cn

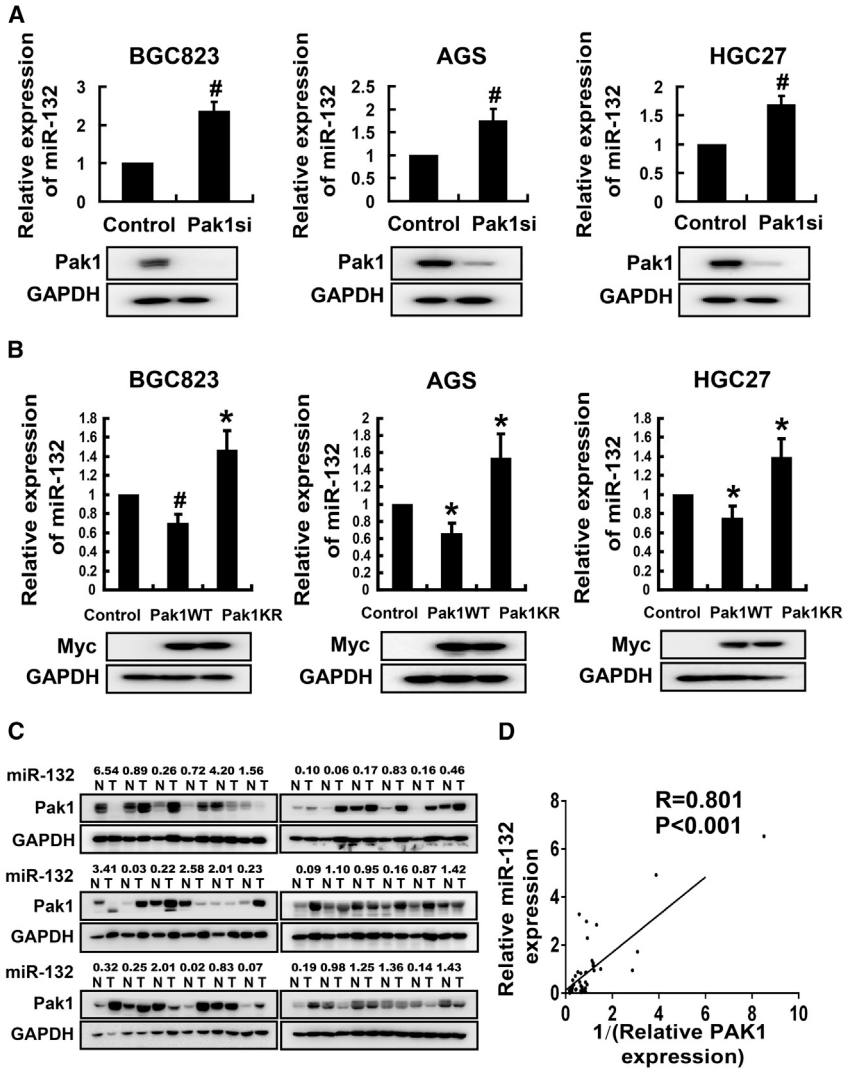

Figure 1. Pak1 Inhibits the Expression of miR-132 in Gastric Cancer Cells

(A) Quantitative real-time PCR was used to analyzed miR-132 expression in BGC823, AGS, and HGC27 cells infected with Pak1-RNAi lentivirus. Pak1 protein expression in the cells was detected by western blot. GAPDH served as protein loading control. (B) Quantitative real-time PCR analysis of miR-132 expression in BGC823, AGS, and HGC27 cells transfected with wild-type Pak1 (Pak1WT) plasmids and kinase-defective mutant Pak1 (Pak1KR) plasmids. Pak1 protein expression was detected with anti-myc antibody. *$p < 0.05$, #$p < 0.01$. (C) Western blot analysis of the protein level of Pak1 in gastric cancer tissues specimens and matched adjacent noncancerous mucosa from 36 (part of 66 patients) representative patients. Relative values of miR-132 expression are shown above the matched samples. T, gastric cancer tissue; N, matched noncancerous adjacent mucosa. (D) Correlation analysis of the relative expression levels of miR-132 and reciprocal Pak1 expression in 43 tissue specimens from gastric cancer patients at stages IIIB, IIIC, and IV. Data in (A) and (B) are presented as mean ± SD.

and metastasis by regulating the Pak1 pathway,[18,19] miRNAs that are regulated by Pak1 kinase have not been explored.

We report here the first evidence of a profound role for miR-132 in metastatic gastric cancer. Interestingly, our studies reveal that miR-132 specifically affects hematogenous metastasis, but not lymph node or implantation metastases. Such selective inhibition of metastasis by miRNA was previously unknown. Subsequently, we show that the expression of miR-132 is regulated by ATF2, which in turn is controlled by Pak1. ATF2 is a new target for Pak1 kinase, and its phosphorylation prevents ATF2 from translocating to the nucleus and thereby reduces the expression of miR-132. We further identify that CD44 and fibronectin1 (FN1) molecules are targets of miR-132 and that miR-132 downregulates their activities to facilitate lymphocytes to home in on cancer cells and kill them via apoptosis. Our studies uncover a novel cell-signaling pathway and a cascade of events (Pak1/ATF2/miR-132/CD44-FN1) that profoundly affect metastasis of gastric cancer and reveal potential targets for therapeutic intervention.

RESULTS

Pak1 Regulates miR-132 Expression in Gastric Cancer

First, we performed miRNA chip analysis (CapitalBio) to identify differentially expressed miRNAs in Pak1-knockdown gastric cancer cells (BGC823; i.e., stable knockdown cell clone).[2] A notable candidate gene we found was miR-132. Its level was significantly higher in Pak1-knockdown cells than in control cells (Figure S1). Subsequently, this result was further validated by quantitative real-time PCR assay. miR-132 expression was markedly increased in Pak1-knockdown BGC823, AGS, and HGC27 cells (Figure 1A). To explore whether this regulation of miR-132 gene expression depends on Pak1 kinase activity, wild-type Pak1 (Pak1WT) or kinase-defective mutant Pak1 (Pak1K299R) plasmids were transiently transfected into BGC823, AGS, and HGC27 cells. Quantitative real-time PCR revealed that Pak1WT decreased miR-132 expression, whereas Pak1KR increased miR-132 expression (Figure 1B), indicating that the regulation of miR-132 expression was dependent on Pak1 kinase activity. These findings were also consistent with the reported theory that Pak1 could be auto-inhibited and auto-activated in a trans-homodimer pattern.[20]

In order to ascertain that Pak1-mediated regulation of miR-132 expression is not just a laboratory phenomenon and that it occurs in human patients with gastric cancer, we obtained tissue specimens from 66 patients and examined them using western blot analysis (Figures 1C and S2). Further analysis showed that there was an inverse

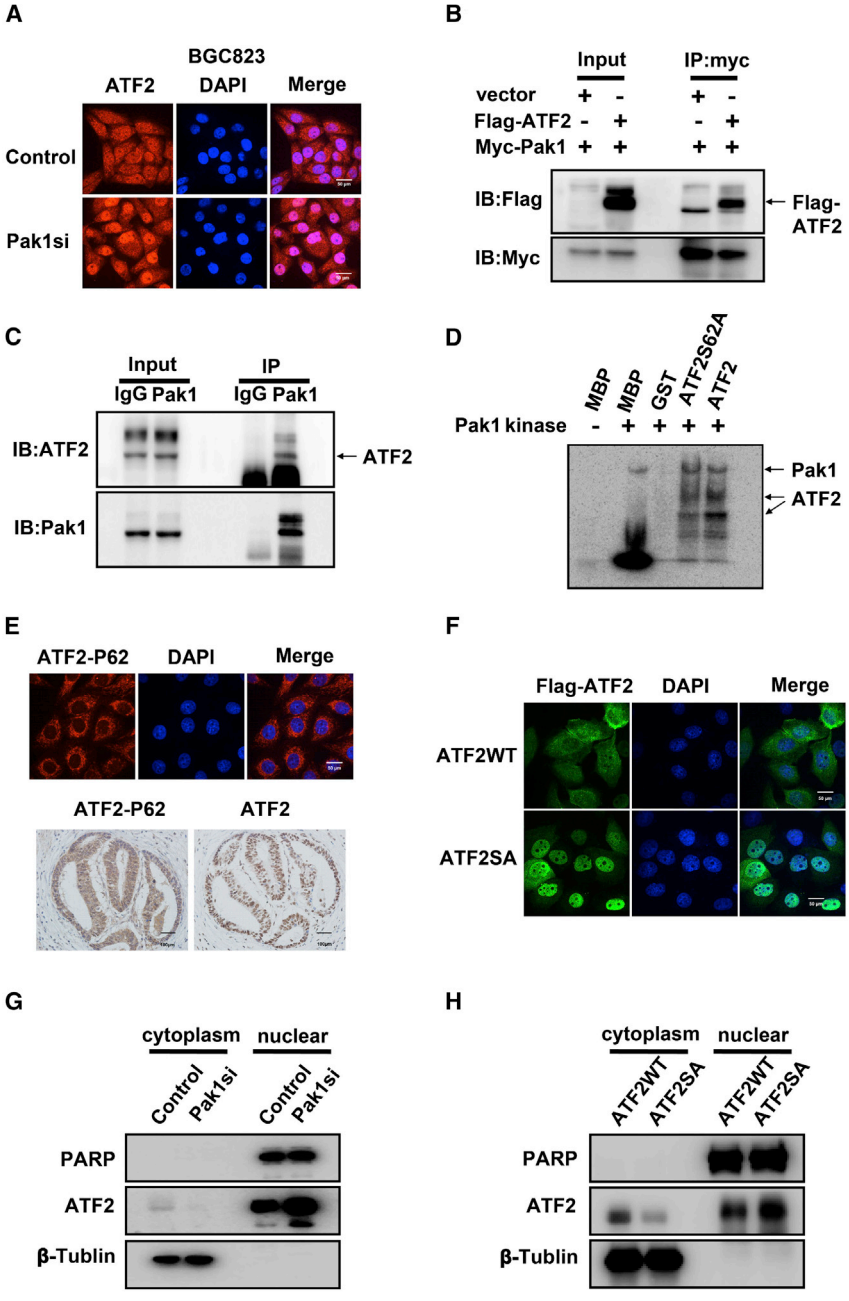

Figure 2. Pak1 Phosphorylates ATF2 on Ser62 and Inhibits ATF2 Translocation into the Cell Nucleus

(A) BGC823 cells were transfected with Pak1-RNAi lentivirus, and the location of ATF2 was analyzed by confocal imaging. (B) FLAG-ATF2 and myc-Pak1 plasmids were co-transfected into BGC823 cells, cell lysates were subjected to immunoprecipitation with myc-specific antibody, and the western blot was probed with FLAG-specific antibody. (C) BGC823 cell lysates were immunoprecipitated with Pak1-specific antibody or IgG and then analyzed by western blot with ATF2 antibody. (D) Kinase assays were performed with purified ATF2 and ATF2S62A protein as substrates for Pak1 kinase. (E) The location of p-ATF2 was examined by confocal imaging assay; p-ATF2 is marked with red and nuclear DNA is marked with blue (top panels). Location of ATF2 and p-ATF2 in paraffin sections of tissues from two gastric cancer patients were evaluated by immunohistochemistry (bottom panels). (F) BGC823 cells were transfected with ATF2WT and ATF2S62A plasmids, and confocal imaging was performed. (G) BGC823 cells were transfected with Pak1-RNAi lentivirus, and protein in cytoplasmic and nuclear extracts was prepared and analyzed by western blot. β-Tubulin and PARP served as cytoplasmic and nuclear protein loading controls, respectively. (H) BGC823 cells were transfected with ATF2WT and ATF2S62A plasmids, and protein in the cytoplasm and nucleus was detected with western blot. All experiments were carried out as described in Materials and Methods.

correlation between the levels of Pak1 and miR132 in advanced gastric cancer tissues (Figure 1D). All of the above results clearly indicate that Pak1 plays a key role in regulating miR-132 expression in gastric cancer.

Pak1 Phosphorylates ATF2 and Inhibits Its Translocation into the Cell Nucleus

A previous study found that the cAMP response element (CRE) motifs on the promoter of miR-132 were important for its expression in neurons.[21] Therefore, we explored whether CREB1 was an agency in Pak1 regulating miR-132 transcription. Western blot showed that Pak1 did not affect expression of CREB1 protein or the level of CREB1 phosphorylation (Figure S3A). Using confocal scanning microscopy, we found that the distributions of CREB1 in the cell cytoplasm and nucleus did not change after the expression of Pak1 was knocked down in gastric cancer cells (Figures S3B–S3D). Studies have shown that Pak1 activates c-Jun N-terminal kinase (JNK) or p38,[22,23] which both in turn phosphorylate ATF2, which is also a CRE-binding protein.[24] These data suggested that Pak1 might regulate miR-132 by affecting the function of ATF2. To prove this hypothesis, we first examined the status of ATF2 in Pak1-knockdown gastric cancer cells. Interestingly, we found that the subcellular distribution of ATF2 was affected in BCG823 gastric cancer cells (Figure 2A). The same study in two more gastric cancer cell lines, AGS and HGC27, also showed very similar results (Figures S4A and S4B). To investigate the potential mechanism of ATF2 subcellular distribution by Pak1, bioinformatics analysis was performed for ATF2 to find potential serine or threonine sites that might be phosphorylated by Pak1. Ser62 was identified as a probable site, suggesting that ATF2 might be directly phosphorylated by Pak1. Pak1, in general, physically interacted with its targets while phosphorylating them. In order to evaluate whether Pak1 directly bound ATF2, we first performed a glutathione S-transferase (GST)-binding

assay. Results showed that in-vitro-translated ATF2 indeed interacted with GST-Pak1; however, in reverse assays, translated Pak1 did not bind with GST-ATF2 (Figures S4C and S4D). In further immunoprecipitation (IP) analysis in BGC823 cells, Myc-tagged Pak1 was able to interact with FLAG-tagged ATF2 (Figures 2B and S4E). In addition, endogenous Pak1 and ATF2 molecules interacted with each other in BGC823 cells (Figures 2C and S4F). All of these results confirmed that Pak1 physically interacted with ATF2. The reason Pak1 could not bind with GST-ATF2 might be because of the GST tag, which might block their interaction, indicating that the N-terminal sequence of ATF2 might be the key region.

Next, we performed in vitro kinase assays to study whether Pak1 phosphorylated ATF2 on Ser62. Pak1 kinase efficiently phosphorylated positive control myelin basic protein (MBP), but it failed to phosphorylate both GST-ATF2 and mutant GST-ATF2S62A containing an alanine substitution at position 62 (Figure S5A). We surmised that the GST tag might be affecting such a process; therefore, we cleaved off the GST tag with PreScission protease. Strikingly, Pak1 efficiently phosphorylated ATF2 (Figure 2D). In this assay, the mutant ATF2S62A was not phosphorylated, indicating that Ser62 was the target for Pak1 kinase. Western blot analysis with phosphorylation antibody against phospho-ATF2 Ser62 confirmed that Pak1 phosphorylated ATF2 in a dose-dependent manner in vitro (Figure S5B). Furthermore, Pak1-knockdown cells, including BGC823, AGS, and HGC27 cells, had decreased levels of phospho-ATF2, whereas overexpressing Pak1 with a transfected Pak1WT vector increased the level of ATF2 phosphorylation in these cells (Figures S5C and S5D).

We then examined whether Pak1 phosphorylation affects subcellular distribution of ATF2 using confocal imaging and immunohistochemistry assays. The results showed that endogenous phospho-ATF2 was mainly located in the cytoplasm (Figure 2E). To assess the role of Ser62 phosphorylation, ATF2WT and ATF2S62A were independently expressed in BGC823 cells. Confocal imaging showed that ATF2S62A accumulated more in the cell nucleus than ATF2WT (Figure 2F). Nucleocytoplasmic separation assays also showed that when Pak1 expression was prevented, ATF2 was predominantly found in the nuclear fraction of BCG823 cells (Figure 2G). Likewise, when BCG823 cells were transfected with mutant Pak1S62A, AFT2 was also predominantly found in the nuclear fraction (Figure 2H). More proof for the same observation was obtained when we performed confocal and western blot analyses in Pak1-knockdown cells. The results showed that constitutively active Pak1 (T423E) promoted ATF2 cytoplasm localization, while ATF2 location did not significantly change in cells transfected with kinase-defective Pak1 (K299R) (Figure S6A). The results were also verified by western blot analyses (Figure S6B).

Overall, our results unequivocally confirmed that Pak1 physically interacts with ATF2 and phosphorylates ATF2 on the Ser62 residue, and this process secludes ATF2 in the cytoplasm. These findings indicate, for the first time, that Pak1 directly regulates ATF2, and this process may lead to reduced ATF2-mediated transcriptional regulation in the nucleus.

ATF2 Regulates miRNA miR-132 Gene Expression in Gastric Cancer Cells

To verify whether ATF2 was the key regulator of miR-132, the potential binding sites of ATF2 were predicted using AliBaba 2 software. As shown in Figure 3A, the promoter sequence contained three potential ATF2-binding CRE sites at positions −30, −469, and −486. To further explore whether ATF2 regulated the expression of miR-132, a quantitative real-time PCR assay was performed, which showed that the expression of miR-132 decreased in gastric cancer cells (BGC823, AGS, and HGC27) when ATF2 was downregulated by ATF2-RNAi-lentivirus (Figure 3B). When ATF2WT or ATF2S62A plasmids were transiently transfected into BGC823, AGS, and HGC27 cells, quantitative real-time PCR revealed that ATF2WT increased expression of miR-132, whereas ATF2S62A did not alter expression (Figure 3C). Chromatin immunoprecipitation (ChIP) and electrophoretic mobility shift assay (EMSA) were carried out to test the binding of ATF2 to the miR-132 promoter. As shown in Figure 3D, the miR-132 promoter sequence −163/+50 (probe A) was bound to ATF2 in the ChIP assay, revealing that ATF2 interacted with the miR-132 promoter at this region. The miR-132 promoter sequence −607 to −518 (probe BC) containing the other two CRE motifs did not immunoprecipitate with ATF2, indicating that these regions were not bona fide targets of ATF2. In further EMSA analyses, nuclear extract from BCG823 cells bound to the sequence between −30 to −39, and the complex was supershifted with ATF2 antibody (Figure 3E). These results confirm that ATF2 interacts with the −30 to −39 region of the miR-132 gene promoter and regulates its expression.

miR-132 Inhibits Adhesion, Migration, and Metastasis of Gastric Cancer Cells

In an attempt to define the role of miR-132 in the invasion and metastasis of gastric cancer cells, we used miR-132-lentivirus to establish stable BGC823, AGS, and HGC27 cell lines to overexpress miR-132. The miR-132 expression level was substantially elevated in these cells (Figure S7). A significant inhibition of adhesion, migration, and invasion ability were observed in all miR-132 overexpressing cells (Figure 4A). All these in vitro results prompted us to investigate whether miR-132 overexpression could inhibit metastasis of gastric cancer cells in vivo. To answer this question, we constructed a cell line, BGC823-luc-miR-132, derived from gastric cancer BGC823 cells stably co-expressing luciferase and miR-132. BGC823-luc-miR-132 cells and control cells expressing luciferase were injected into two separate groups of nude mice through tail veins. Live animal bioluminescence imaging (BLI) was used to detect tumor growth and onset of metastases. Thirty minutes after injection of the cancer cells, equal bioluminescence existed in mice lungs. The mice were imaged each week, and the final images taken just before they died are shown in Figure 4B. Mice injected with BGC823-luc-miR-132 cells showed no marked decrease in pulmonary metastasis when compared with mice injected with control

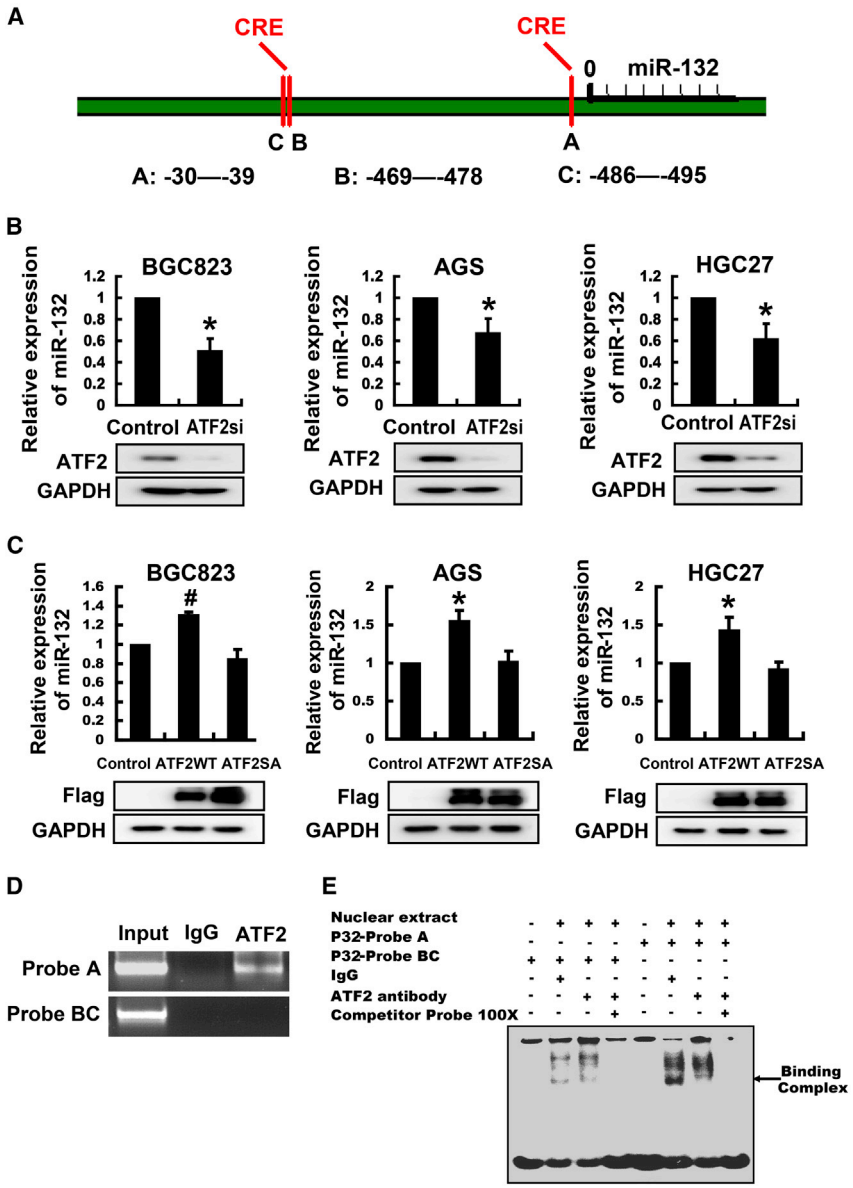

Figure 3. ATF2 Modulates miR-132 Transcription by Binding to the –30 to –39 Region of Its Promoter

(A) Potential ATF2-binding CRE sites in the ATF2 promoter region were predicted with Alibaba software. (B) miR-132 expression in BGC823, AGS, and HGC27 cells transfected with ATF2-RNAi lentivirus was examined using quantitative real-time PCR. ATF2 protein expression in these cells was measured by western blot. (C) Quantitative real-time PCR analysis was preformed to examine miR-132 expression in BGC823, AGS, and HGC27 cells transfected with ATF2WT and ATF2SA plasmids. ATF2 protein expression in cells was detected using FLAG antibody by western blot. (D) A ChIP assay was used to study the binding of ATF2 to the miR-132 promoter. (E) The binding of ATF2 to the miR-132 −30 to −39 promoter sequence was examined by EMSA. Data in (B) and (C) are presented as mean ± SD, and detailed experiments were performed as described in Materials and Methods. *$p < 0.05$.

cells. However, in the control group, four out of ten mice exhibited brain metastasis, and another three mice had bone metastasis, whereas none of the mice in the BGC823-luc-miR-132 group had brain or bone metastasis. H&E staining confirmed that the metastases detected by BLI were in brain or bone (Figure 4C). In addition, the survival rate of mice injected with BGC823-luc-miR-132 cells was significantly higher than that of control group ($p < 0.05$) (Figure 4D).

CD44 and FN1 Are Potential Targets for miR-132 in Gastric Cancer

We searched for potential targets of miR-132 to uncover its mechanism of action and determine whether miR-132 contributes to gastric cancer metastasis. Subsequently, a bioinformatics TargetScan algorithm was used to analyze the targets of miR-132. Of the various candidates we identified, CD44 and FN1 stood out, because both are known to be involved in cancer metastasis. To investigate whether CD44 and FN1 are direct targets of miR-132, we constructed dual-luciferase reporter vectors containing CD44 or FN1 3′ UTR mRNA (pMIR REPORT-CD44-3′-UTR and pMIR REPORT-FN1-3′-UTR). pMIR REPORT-CD44-MUT and pMIR REPORT-FN1-MUT vectors with mutation target sites were also constructed. The plasmids were independently co-transfected with miRNA mimics into BGC823 and HGC27 cells. Results revealed the luciferase activity of pMIR REPORT-CD44-3′-UTR and pMIR REPORT-FN1-3′-UTR reporters was significantly suppressed, but the luciferase activity of pMIR REPORT-CD44-MUT and pMIR REPORT-FN1-MUT reporters was unchanged (Figures 5A and 5B). Using western blot analysis, we examined protein levels of CD44 and FN1 in gastric cancer cells with miR-132 overexpression, Pak1 knockdown, or ATF2 overexpression. A significant reduction in the levels of the endogenous CD44 and FN1 protein was observed in all these cells (Figures 5C–5E). To further assess the role of miR-132-mediated inhibition of CD44 and FN1 protein expression in gastric cancer patients, we examined the expression of miR-132 and protein levels of CD44 and FN1 in 102 gastric cancer tissue specimens. Figure S8 shows the levels of CD44 and FN1 protein in 102 representative patients. Further results showed an inverse relationship between miR-132 and CD44 in advanced cancer tissues (Figure 5F). Although this relationship between miR-132 and FN1 was not significant in these advanced cancer tissues

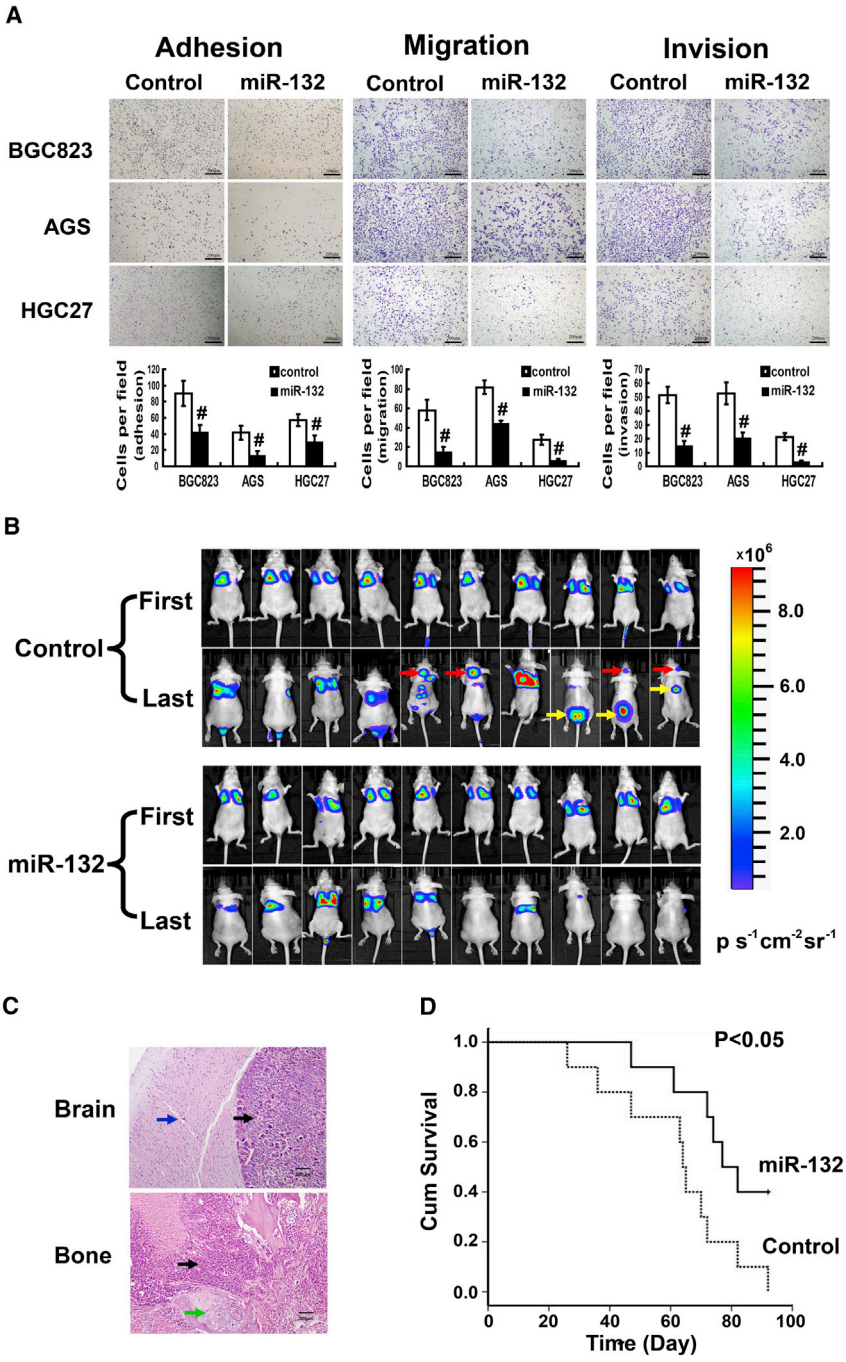

Figure 4. miR-132 Overexpression Inhibits Adhesion, Migration, and Metastasis of Gastric Cancer Cells

(A) Cell adhesion, migration and invasion assays were performed to evaluate the effect of miR-132 on BGC823, AGS, and HGC27 cells. Representative photomicrographs of the results were taken at original magnification ×100. The cell number was counted in 20 independent symmetrical microscopic visual fields (at original magnification ×400). Data are presented with mean ± SD; #$p < 0.01$. (B) Tumor metastasis burden of xenografted animals was monitored weekly using BLI. "First" represents images taken 30 min after injection of cancer cells. "Last" represents images taken before death. (C) The brain and bones were excised, embedded in paraffin, and stained with H&E. The black arrow points to tumor tissue, and the blue arrow or green arrow points to normal brain or bone tissues, respectively. (D) Kaplan-Meir survival curves of control and miR-132 overexpressing groups were analyzed using GraphPad Prism software.

(data not shown), a reverse relationship between miR-132 and FN1 was found in 14 metastatic cancer tissues (Figure 5G). These results indicate that CD44 and FN1 are regulated directly by miR-132 in a negative manner in gastric cancer. We also explored whether other previously reported targets of miR-132, such as Sirt1, SOX4, brain-derived neurotrophic factor (BDNF), HBEGF, and MAPK1, participate in gastric cancer metastasis. Western blot analyses showed that the expression of Sirt1 and BDNF was also reduced in miR-132 overexpressing BGC823 and AGS cells, suggesting that Sirt1 and BDNF may also be involved in miR-132-mediated inhibition of gastric cancer metastasis (Figure S9).

miR-132 Enables Lymphocytes to Home In on Gastric Cancer Cells and Kill Them by Inducing Apoptosis

Because CD44 and FN1 were previously reported to be involved in lymphocyte homing and play important roles in immune evasion,[25,26] we investigated whether miR-132 participates in immune evasion. Interaction between lymphocytes (isolated from human whole blood) and gastric cancer cells was observed by live-cell imaging system, and the effect of lymphocytes on cancer cells were assessed using an MTT assay. Results demonstrated that compared with control cells, cells stably expressing miR-132 were surrounded by numerous lymphocytes and easily killed (Figures 6A–6D; Movies S1 and S2). Annexin-V-mediated apoptosis detection showed that apoptosis was induced in BGC823 cells overexpressing miR-132 (Figures 6E and 6F). These results indicate that miR-132 regulates immune evasion and destruction of gastric cancer cells by inducing apoptosis.

Low Expression of miR-132 in Gastric Cancer Cells Is Associated with Poor Prognosis and Elevated Hematogenous Metastasis

Finally, we analyzed the expression level of miR-132 in cancer tissues and matched adjacent noncancerous tissues from 201 gastric cancer

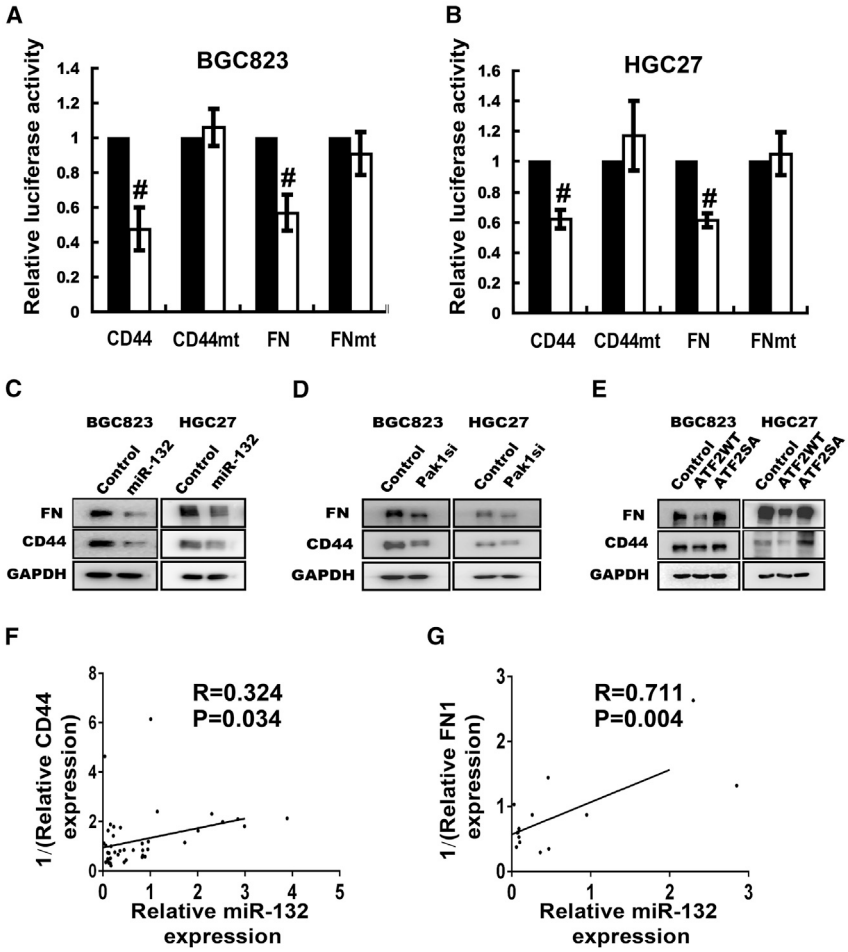

Figure 5. CD44 and FN1 Are Potential Targets of miR-132

(A and B) miR-132 mimics or control mimics were co-transfected with luciferase vectors, and the luciferase activity of CD44, FN1, CD44-MUT, and FN1-MUT was measured. Data are presented with mean ± SD; #$p < 0.01$. (C) Western blot was used to examine protein levels of CD44 and FN1 in BGC823 and HGC27 stable cell lines. (D) Protein levels of CD44 and FN1 in BGC823 and HGC27 cells transfected with Pak1-RNAi lentivirus were detected by western blot. (E) Western blot was performed to evaluate the protein levels of CD44 and FN1 in BGC823 and HGC27 cells transfected with ATF2WT and ATF2S62A plasmids. (F) Correlation analysis was performed to examine the correlation between miR-132 and reciprocal CD44 expression in 43 cancer tissues at advanced stages IIIB, IIIC, and IV. (G) Correlation analysis of the relative expression levels of miR-132 and reciprocal FN1 expression in 14 gastric cancer tissues with hematogenous metastasis before the operation or within 5 years after surgery. All experiments were carried out as described in Materials and Methods.

patients by quantitative real-time PCR. miR-132 expression level was significantly reduced in the tumor tissues compared with the adjacent normal mucosa tissues (Figure 7A). As shown in Table 1, miR-132 expression in tumor tissues was not significantly associated with gender, tumor location, gross type, lymph node status, lymph node metastasis, lymphatic invasion, or implantation metastasis. However, miR-132 expression was significantly correlated with age ($p = 0.036$), tumor size ($p = 0.001$), histological type ($p = 0.003$), depth of invasion ($p = 0.007$), venous invasion ($p = 0.002$), hematogenous metastasis ($p = 0.022$), and pathological stage ($p = 0.041$). The 5-year survival rate of the miR-132 high-expression group was significantly better than that of the low-expression group ($p < 0.01$) (Figure 7B). In addition, multivariate analysis showed that miR-132 expression was an independent risk factor for overall survival (Table S1). The expression of miR-132 was lower in hepatic metastases of gastric cancer than that in primary tumor. However, miR-132 expression in lymphatic and implanted metastases of gastric cancer was not significantly different from primary tumor (Figures 7C and 7D). In order to further confirm that miR-132 was involved in hematogenous metastasis, we analyzed the expression of miR-132 in a metastatic colorectal data from the GEO database. Consistent with the data for gastric cancer tissue, expression of miR-132 was markedly downregulated in hepatic metastases compared with primary colorectal tumors (Figure 7E), indicating that miR-132 may be an important hematogenous metastasis factor in gastrointestinal carcinoma.

DISCUSSION

Pak1 belongs to a family of kinases that transduce signals elicited on the cell surface and modulate critical cytoplasmic and nuclear functions.[8] Pak1 is a prototype of group I Pak family, and its aberrant regulation has been shown to be the cause of several oncogenic processes. Our previous studies consistently pointed to a crucial role for Pak1 in gastric cancer progression and metastasis.[2] Recently, several studies have shown that Pak1 is an important target gene of the miRNA signaling pathway. In breast cancer cells, the expression and function of Pak1 is regulated by miR-7.[19] Moreover, regaining miR-145 and miR-221 expression markedly suppresses bladder cancer cell invasion and endothelial progenitor cell growth by targeting Pak1.[27,28] In gastric cancer, we demonstrated that miR-133a could inhibit tumor proliferation and invasion by targeting the CDC42/Pak1 pathway.[18] However, there are few reports of miRNAs that are regulated by Pak1. In this study, we first identified miR-132 as a gene downstream of Pak1 by performing miRNA microarray analysis. Further experiments revealed that Pak1 could downregulate miR-132 in a kinase-dependent manner and that increased expression of Pak1 in gastric cancer tissues is negatively correlated with miR-132 levels.

ATF2, a member of the b-ZIP family of transcription factors, plays crucial roles in cellular development and survival.[29] Transcriptional activity of ATF2 is regulated by p38, JNK, and extracellular

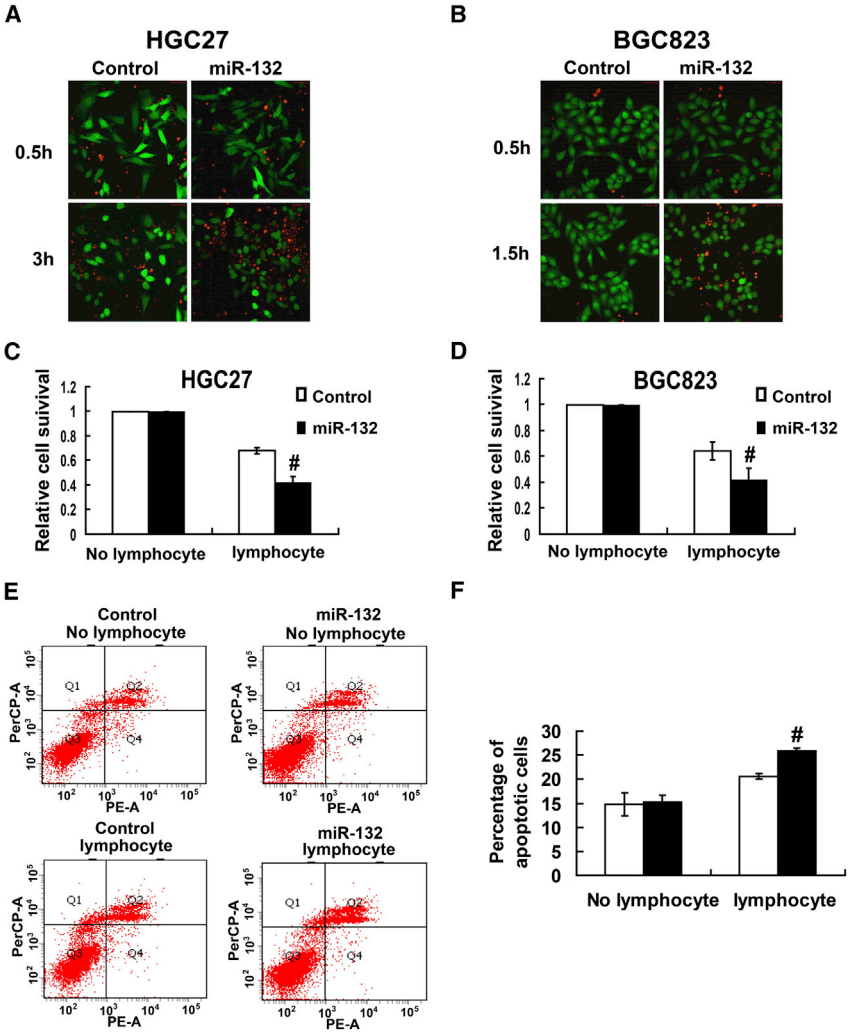

Figure 6. miR-132 Promotes Lymphocytes to Home In on Gastric Cancer Cells and Attack Them by Inducing Apoptosis

(A and B) Gastric cancer cells overexpressing miR-132 or control cells were labeled with green fluorescent protein and incubated with lymphocytes that were marked with red fluorescent protein. Live-cell images taken at 0.5 hr, 1.5 hr, and 3 hr are shown. (C and D) HGC27 and BGC823 cells overexpressing miR-132 or control cells were incubated with lymphocytes for 24 hr and subsequently washed and incubated with 10 μL MTT (5 mg/mL) for 4 hr, and cell vitality was measured. (E and F) Tumor cells and lymphocytes were co-incubated for 24 hr, and apoptotic cells were analyzed using an Annexin V apoptosis detection kit. Data were analyzed using GraphPad prism and are presented as mean ± SD; #$p < 0.01$ All experiments were carried out as described in Materials and Methods.

signal-regulated kinase (ERK). These kinases activate ATF2 by phosphorylating threonine residues Thr69 and Thr71.[30] ATF2 is also activated by human vaccinia-related kinase 1 (VRK1) by phosphorylating Ser62 and Thr73.[31] Although some studies demonstrate that ATF2 performs oncogenic functions in some tumors, such as melanoma, models of breast and skin tumors also revealed that ATF2 has a tumor suppressive function.[32] A recent study found that ATF2 plays a key role in dissemination and metastasis in mammary cancer.[33] Here, we found that Pak1 controls ATF2 transcriptional activity in an intriguing way, by phosphorylating its Ser62 residue and preventing it from entering the nucleus. Further experiments reveal that ATF2 regulates miR-132 transcription by binding to the −30 to −39 region of its promoter.

Our in vitro studies show that miR-132 inhibits cell adhesion, migration, and invasion, and in vivo observations demonstrate that it prevents hematogenous metastasis of gastric cancer cells. CD44 is a class I integral membrane glycoprotein that interacts with various other extracellular matrix components and has been linked to the metastatic potential of a variety of human cancers.[34,35] FN1 is a large multi-domain cellular and extracellular matrix (ECM) glycoprotein and is associated with tumor angiogenesis and metastasis.[36] In this study, we identify CD44 and FN1 as novel targets for miR-132, indicating that miR-132 may inhibit the hematogenous metastasis of gastric cancer cells by regulating CD44 and FN1. Our data also show that previously reported targets of miR-132, Sirt1,[37,38] and BDNF[39] may be involved in the hematogenous metastasis of gastric cancer. However, additional studies are needed to confirm their roles.

miRNAs have been shown to modulate the innate and adaptive immune responses and immune cell repertoire in the tumor microenvironment.[40,41] miRNAs regulate T cell responses, maturation, and differentiation and affect tumor cell immune evasion.[42] For example, miR-222 and miR-339 promote the resistance of cancer cells to cytotoxic T lymphocytes by downregulating intercellular adhesion molecule 1 (ICAM-1).[43] Several studies have demonstrated that CD44 and FN1 affect lymphocyte homing and facilitate immune evasion.[25,26] Our study is the first to prove that miR-132 promotes the process by which lymphocytes encircle gastric cancer cells and destroy them by inducing apoptosis. However, the effects of miR-132, CD44, and FN1 on lymphocytes, immune evasion, and hematogenous metastasis of gastric cancer cells need further investigation to identify the mechanisms involved.

Previous studies have documented that miR-132 participates in inflammation and neural development.[44,45] Recently, several studies have reported differential expression of miR-132 in some tumors, including downregulation in colorectal cancer, breast

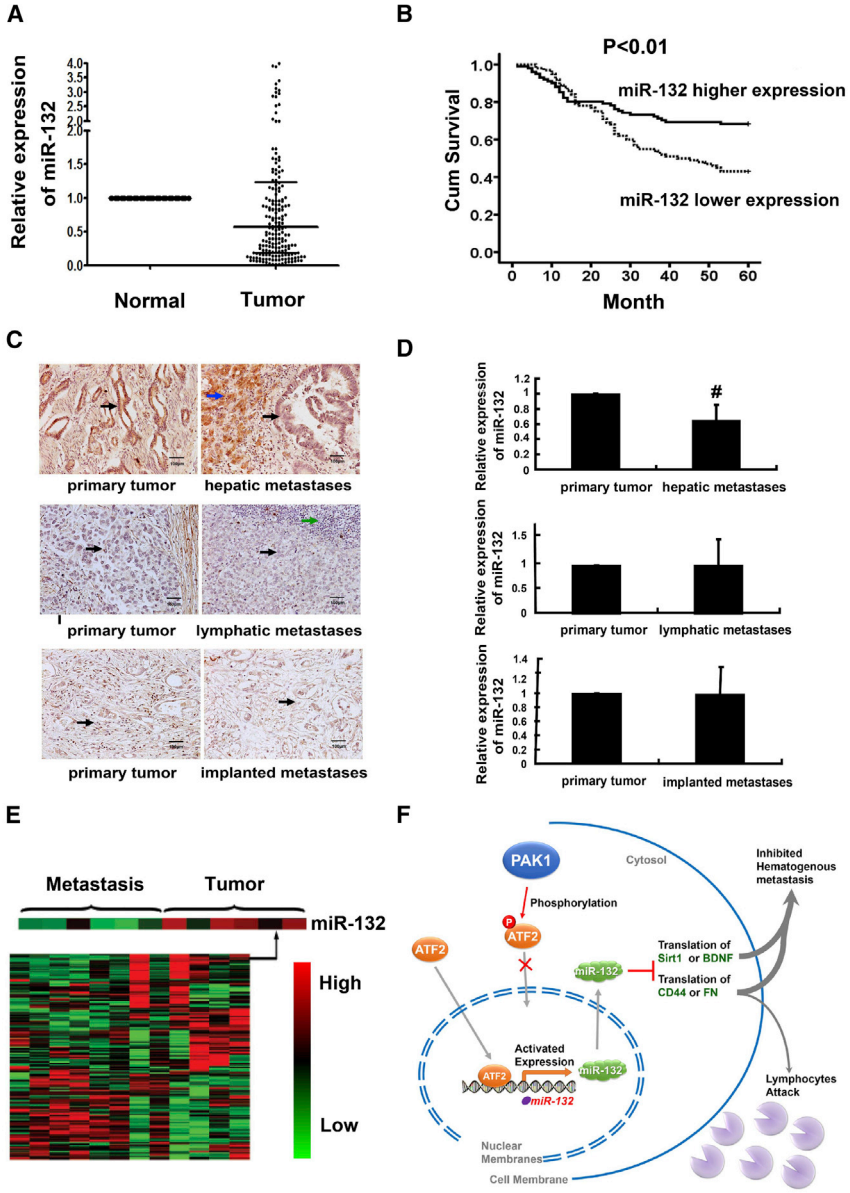

Figure 7. Downregulation of miR-132 Expression in Gastric Cancer Cells Is Associated with Poor Prognosis and Elevated Hematogenous Metastasis

(A) Quantitative real-time PCR was performed to detect the expression level of miR-132 in gastric cancer tissues and matched adjacent noncancerous mucosa from 201 patients, and the expression of miR-132 in cancer tissues was normalized by its adjacent noncancerous tissue (mean with 95% CI). (B) Kaplan-Meir survival curves of the miR-132 lower expression group and the miR-132 higher expression group. The cutoff value for miR-132 expression was defined as 0.57-fold. (C) miR-132 expression in 20 hepatic metastases, 40 lymphatic metastases, and 21 implanted metastases of gastric cancer and matched primary tumors was detected using an in situ hybridization assay. Black arrows point to tumor tissue, the blue arrow points to hepatic tissue, and the green arrow points to lymphatic tissue. (D) Statistical analysis with the relative expression of miR-132 (mean ± SD). #$p < 0.01$. (E) Differences in miR-132 expression between hepatic metastases and primary colorectal tumors were obtained from the published expression dataset GEO: GSE54088 and re-analyzed using R software. (F) Proposed model of the Pak1/ATF2/miR-132/CD44-FN1/Sirt1/BDNF signaling pathway.

cancer, non-small cell lung cancer, osteosarcoma, and prostate cancer and upregulation in glioma and pancreatic cancer.[46–50] A study by Liu et al.[50] revealed that miR-132 was overexpressed in gastric cancer tissue from 79 patients, and expression levels of miR-132 were positively associated with the frequency of lymph node metastasis. In contrast, our results show that miR-132 expression levels are significantly downregulated in gastric cancer and correlated with hematogenous metastasis rather than lymph node metastasis. Gastric cancer patients with hematogenous metastasis usually have a poor prognosis.[15,51] Until now, only a few genes have been reported to specifically affect the hematogenous metastasis of gastric cancer while having no role in lymph node metastasis or implantation metastasis. The strong link between miR-132 and hematogenous metastasis of gastric cancer cells, as shown in our study, may point to a new potential therapeutic target.

In our model of the Pak1/ATF2/miR-132/CD44-FN1 signal transduction pathway and cascade of events in gastric cancer oncogenesis (Figure 7F), Pak1 interacts with ATF2 and phosphorylates the Ser62 residue, which prevents ATF2 translocation into the cell nucleus and reduces ATF2-mediated transcriptional regulation. Nuclear ATF2 binds to the promoter of miR-132, induces gene expression, downregulates CD44/FN1/Sirt1/BDNF, and recruits lymphocytes to attack gastric cancer cells to inhibit hematogenous metastasis. However, in gastric cancer patients, miR-132-mediated suppression of hematogenous metastasis is affected, because of ATF2 is secluded in the cytoplasm by Pak1 kinase activity.

MATERIALS AND METHODS

Gastric Cancer Cell Lines

BGC823, AGS, and HGC27 human gastric cancer cells were purchased from the Cell Bank of Type Culture Collection of Chinese Academy of Sciences. A short tandem repeat DNA test was performed for cell line authentication. BGC823 and AGS cells were cultured in DMEM medium supplemented with 10% fetal bovine serum (FBS) and HGC27 cells in RPMI 1640 medium supplemented with 10% FBS (Gibco).

Table 1. Association between miR-132 Expression and Clinicopathologic Features in Patients with Gastric Cancer

	Parameters	No. of Patients	Change in miR-132 Expression[a]	p Value[b]
Age (y)	<65	130	0.70 (0.23–1.39)	0.036
	≥65	71	0.40 (0.14–0.96)	
Gender	male	153	0.63 (0.21–1.21)	0.300
	female	48	0.31 (0.14–1.36)	
Location	upper third	14	0.48 (0.26–1.02)	0.426
	middle third	32	0.60 (0.25–2.05)	
	lower third	113	0.70(0.17–1.29)	
Gross type	extensive	42	0.41 (0.13–1.03)	0.571
	localized	29	0.47 (0.10–1.66)	
	infiltrative	172	0.59 (0.19–1.22)	
Size (maximal diameter)	<5 cm	89	0.87 (0.31–1.43)	0.001
	≥5 cm	112	0.39 (0.14–0.99)	
Histological type	intestinal	89	0.89 (0.26–1.70)	0.003
	diffuse	112	0.46 (0.16–0.88)	
Depth of invasion (pT)	T_1, T_2, T_3	130	0.73 (0.24–1.42)	0.007
	T_4	71	0.45 (0.14–0.84)	
Lymph node status (pN)	N_0, N_1	94	0.57 (0.20–1.15)	0.732
	N_2, N_3	107	0.57 (0.18–1.36)	
Lymph node metastasis	no	57	0.64 (0.20–1.25)	0.886
	yes	144	0.55 (0.18–1.24)	
Lymphatic invasion	no	154	0.63 (0.22–1.26)	0.236
	yes	47	0.45 (0.11–1.01)	
Venous invasion	no	193	0.60 (0.22–1.27)	0.002
	yes	8	0.09 (0.06–0.33)	
Hematogenous metastasis[c]	no	181	0.64 (0.21–1.34)	0.022
	yes	20	0.32 (0.11–0.57)	
Implantation metastasis	no	189	0.57 (0.18–1.24)	0.890
	yes	12	0.54 (0.22–1.49)	
Pathological stage	I–IIIb	160	0.65 (0.22–1.35)	0.041
	IIIc and IV	41	0.32 (0.17–0.92)	

[a]Median of relative expression, with 25th–75th percentile in parentheses.
[b]Mann-Whitney test (for two groups) or Kruskal-Wallis test (for more than two groups).
[c]Hepatic metastasis, pulmonary metastasis, bone metastasis, and brain metastasis occurrence before the operation or within 5 years after the operation.

Gastric Cancer Tissue Specimens

The present study included tissue specimens from 201 patients with gastric cancer who underwent surgery in our hospital from March 2007 to November 2008. Fresh samples of gastric cancer tissue and adjacent noncancerous mucosa were harvested and immediately frozen in liquid nitrogen. The use of human tissues was approved by the Medical Ethics and Human Clinical Trial Committee of the First Affiliated Hospital of China Medical University.

Western Blot Analysis and Immunoprecipitation

Total protein from gastric cancer cells and tissues were isolated with RIPA lysis buffer (Beyotime), and cytosolic and nuclear protein fractions were purified with a nuclear and cytoplasmic protein extraction kit (Beyotime). Western blot analysis and immunoprecipitation were performed as previously described.[52] The intensity of the bands in western blot analysis was quantified using ImageJ (NIH). Antibodies against CD44, Sirt1, ATF2, Pak1, and PARP were purchased from Cell Signaling Technology, P-ATF2 ser62 antibody was from Abnova, and mouse anti-myc and anti-FLAG monoclonal antibody were from Abmart. Rabbit anti-SOX4, anti-BDNF, anti-HBEGF, anti-MAPK1, and anti-β tubulin were purchased from Abcam, and mouse anti-GAPDH was purchased from KangCheng Bio.

Immunofluorescence and Confocal Imaging

Gastric cancer cells were seeded on glass coverslips in six-well plates. After 24 hr, the cells were fixed in 4% paraformaldehyde and then blocked with normal goat serum. Cells were incubated overnight at 4°C with primary antibody, washed with PBS with1‰ Triton X-100, and incubated with secondary antibody conjugated with 488 nm or 594 nm dye (Invitrogen). DNA was stained by DAPI (Sigma). Confocal scanning analysis was performed with a Leica SP2AOBS confocal microscope.

Kinase Assay

The Pak1 kinase assay was performed as described previously.[53] Recombinant Pak1 kinase and ATF2 protein were used for the assay. ATF2 and positive control myelin basic protein (MBP) (Invitrogen) were exogenous substrates for Pak1 kinase (Invitrogen). Phosphorylated proteins were separated on SDS-PAGE and analyzed by autoradiography.

Quantitative Real-Time PCR

Quantitative real-time PCR was performed using the stem-loop quantitative real-time PCR method. Total RNA was reversely transcribed using the miR-132 reverse transcriptase primer 5′-GTCGTAT CCAGTGCAGGGTCCGAGGTATTCGCACTGGATACGACCGAC CA-3′ and the U6 reverse transcriptase primer 5′-AACGCT TCAC GAATTTGCGT-3′. The following PCR primers were used: miR-132, forward 5′-GTGCAGGGTCCGAGGT-3′, reverse 5′-GCCGTAACA GTCTACAGCCATG-3′; U6, forward 5′-CTCGCTTCGGCAGCA CA-3′, reverse 5′-AAC GCTTCACGAATTTGCGT-3′. miR-132 levels were determined using the $2^{-\Delta\Delta Ct}$ method.

Microarray Profiling

miRNA chip analysis of stable Pak1-knockdown gastric cancer BGC823 cells and control cells was performed by CapitalBio.

Lentiviral Production and Establishment of Stable Expression Cell Lines

miR-132-lentivirus, Pak1-RNAi lentivirus, and ATF2-RNAi lentivirus were purchased from Shanghai GeneChem. The pre-miR-132 sequence was 5′-CCGCCCCCGCGUCUCCAGGGCAACCGUGGC UUUCGAUUGUUACUGUGGGAACUGGAGGUAACAGUCUAC AGCCAUGGUCGCCCCGCAGCACGCCCACGCGC-3′, and the control sequence for miR-132 was 5′-TTCTCCGAACGTGUCAC GT-3′ with a skeleton of miR-30. Both control and miR-132 lentivirus had a GFP gene and a puromycin resistance gene. The small hairpin RNA (shRNA) Pak1 sequence was 5′-CTAAGAGGTGAACATG TAT-3′, the shRNA ATF2 sequence was 5′-GGCTATCATACTGCT GATA-3′, and the control shRNA sequence for shRNA was 5′-TTC TCCGAACGTGUCACGT-3′. Gastric cancer cells were plated in six-well plates and infected with the lentivirus according to the manufacturer's instruction. Transduced cells were selected in medium containing 4 μg/mL puromycin (Sigma) for 2 weeks before phenotypic and functional analyses.

Immunohistochemistry

Localization of ATF2 and p-ATF2 Ser62 proteins was done via immunohistochemistry using 4-μm paraffin sections of gastric cancer tissue. The sections were deparaffinized, rehydrated, and heated for antigen retrieval and to block endogenous peroxidases. Nonspecific binding was blocked by incubating the slides with normal goat serum for 1 hr at room temperature. The sections were incubated overnight at 4°C with ATF2 (Cell Signaling Technology) or p-ATF2 Ser62 (Abnova) primary antibody and then detected with the EliVision plus kit and a 3′3-diaminobenzidine (DAB) kit (MaiXin.Bio).

Luciferase Assay

Gastric cancer cells stably overexpressing miR-132 were seeded and grown in 24-well plates. At 70% confluence, the cells were transiently cotransfected with a luciferase reporter construct and control pRL-TK plasmid. After 24 hr, cells were harvested with passive lysis buffer, and luciferase activity was determined using the Dual-Luciferase Assay System (Promega). pRL-TK activity was used to normalize the transfection. Each assay was performed in triplicate.

ChIP

BGC823 cell extract was subjected to ChIP assay using a ChIP assay kit (Upstate Biotechnology) according to the manufacturer's instructions. The DNA pulled down by ATF2 antibody or immunoglobulin G (IgG) was amplified by PCR. The following primer pairs were used: CRE (probe A), forward 5′-CTGTCCGCGGTGCTGATCAACG-3′, reverse 5′-AAGCCACGGTTGCCCTGGAGAC-3′ (which amplifies the miR-132 promoter region containing one CRE motif [−163/+50]); and CRE (probe BC), forward 5′-GCCTCTGCGAGCGGAGCTGT-3′, reverse 5′-GGGCAGTAAGCAGTCTAGAGCCAAGG-3′ (which amplifies another miR-132 promoter region containing two CRE motifs [−607/−518]).

EMSA

The binding sequences of the miR-132 promoter encompassing the −30 to −39 region, 5′-CGCCCCCCCGCGGCCCTGACGTCA GCCCGCC-3′ and 5′-GGCGGGCTGACGTCAGGGCCGCGGGG GGGCG-3′, were synthesized with 3′ overhangs, annealed, and end labeled with digoxigenin (DIG) (second-generation DIG gel shift kit, Roche). Nuclear extract from BGC823 cells was used in EMSAs. Supershift assays were performed by pre-incubating the nuclear extract with 1 μL ATF2 antibody (Santa Cruz Biotechnology) at room temperature for 20 min before adding DNA probes.

Cell Adhesion Assay

Gastric cancer cells were seeded onto FN1-coated (BD Biosciences) 12-well plates. After incubation in a 5% CO_2 incubator for 30 min, non-adherent cells were removed by gently washing twice with PBS. The adhesive cells were fixed with 4% paraformaldehyde in PBS at 4°C for 10 min and then stained with 0.4% trypan blue (Beyotime) and counted under microscopy.

Cell Migration and Invasion Assays

Cell migration and invasion assays were performed using Matrigel-coated (for the invasion assay) (BD Biosciences) or uncoated (for the migration assay) 24-well transwell plates (Corning, 8 μm pore size). Gastric cancer cells in culture medium containing 1% FBS were seeded in the upper chamber, and culture medium containing 20% FBS filled the lower chamber. After 24 hr, the cells from the upper chamber were removed with a cotton swab, and the transwell membrane was fixed, stained, photographed, and counted. All assays were performed in triplicate.

Mouse Metastasis Model and Live Imaging

1×10^6 BGC823 cells constitutively overexpressing miR-132-luciferase or control cells were injected into 6-week-old null mice via tail vein (ten mice per group). For quantitative evaluation of dissemination in mice body and tumor growth, 150 mg/kg D-Luciferin (PerkinElmer) was injected into the peritoneum before live imaging. Images were obtained by live-animal BLI (PerkinElmer) once per week. All experiments were conducted according to the guidelines for animal care and use of China, and they were approved by the animal ethics committee of China Medical University

Live Imaging of Interaction of Lymphocytes with Gastric Cancer Cells

Lymphocytes were isolated from whole blood of normal human using a Ficoll-Paque PLUS kit (GE Healthcare). Lymphocytes were labeled with a red fluorescence probe (Invitrogen), gastric cancer cells were marked by green fluorescence (Invitrogen), and the two types of cells were co-cultured. An Ultra VIEW VoX spinning disk confocal live-cell imaging system (Olympus) was used to observe the interaction between lymphocytes and gastric cancer cells.

In Situ Hybridization

An in situ hybridization assay for miR-132 was performed according to the manufacturer's protocol (Boster Bio-Engineering). 4-μm

sections were hybridized with a DIG-modified miRNA probe: 5′-CG ACCATGGCTGTAGACTGTTA-3′. Two experienced pathologists independently scored the results by microscopy based on the intensity and proportion of positive cells.

Statistical Analysis

The relationship between miR-132 expression and clinical features was analyzed using a Kruskal-Wallis rank test and Mann-Whitney test. Survival outcome was illustrated by Kaplan-Meier curves, and survival differences between groups were analyzed with log-rank tests. All phenotypes of cells were analyzed by Student's test. All statistical analyses were preformed using SPSS 16.0, and $p < 0.05$ was considered significant.

ACCESSION NUMBERS

The accession number for the microRNA microarray data reported in this paper is GEO: GSE84298. Microarray data for metastatic colorectal cancers (GEO: GSE54088) were obtained from the GEO.[54]

SUPPLEMENTAL INFORMATION

Supplemental Information includes nine figures, one table, and two movies and can be found with this article online at http://dx.doi.org/10.1016/j.omtn.2017.07.005.

AUTHOR CONTRIBUTIONS

Feng Li conceived and designed the study. Funan Liu and Z.C. performed most cell and animal experiments and drafted the manuscript. Funan Liu and H.X. collected clinical specimens and patient clinicopathological data. Y.L. and H.Z. conducted the statistical analysis. J.L. and Furong Liu performed confocal and live-cell imaging. X.L. performed the kinase assay. All authors read, revised, and approved the final manuscript.

CONFLICT OF INTEREST

The authors declare no conflict of interest.

ACKNOWLEDGMENTS

This study was supported by the National Natural Science Foundation of China (grants 31000627, 31371424, 31571457, 81001092, and 81230077), the Natural Science Foundation of Liaoning Province (grant 2013021097), the Basic Research Project of Education Department of Liaoning Province (grant LZ2015071), and the Ministry of Education of China (grant IRT 13101).

REFERENCES

1. Kelly, M.L., and Chernoff, J. (2011). Getting smart about p21-activated kinases. Mol. Cell. Biol. *31*, 386–387.
2. Liu, F., Li, X., Wang, C., Cai, X., Du, Z., Xu, H., and Li, F. (2009). Downregulation of p21-activated kinase-1 inhibits the growth of gastric cancer cells involving cyclin B1. Int. J. Cancer *125*, 2511–2519.
3. Adam, L., Vadlamudi, R., Kondapaka, S.B., Chernoff, J., Mendelsohn, J., and Kumar, R. (1998). Heregulin regulates cytoskeletal reorganization and cell migration through the p21-activated kinase-1 via phosphatidylinositol-3 kinase. J. Biol. Chem. *273*, 28238–28246.
4. Wang, R.A., Vadlamudi, R.K., Bagheri-Yarmand, R., Beuvink, I., Hynes, N.E., and Kumar, R. (2003). Essential functions of p21-activated kinase 1 in morphogenesis and differentiation of mammary glands. J. Cell Biol. *161*, 583–592.
5. Kumar, R., Gururaj, A.E., and Barnes, C.J. (2006). p21-activated kinases in cancer. Nat. Rev. Cancer *6*, 459–471.
6. Molli, P.R., Li, D.Q., Murray, B.W., Rayala, S.K., and Kumar, R. (2009). PAK signaling in oncogenesis. Oncogene *28*, 2545–2555.
7. Vadlamudi, R.K., Bagheri-Yarmand, R., Yang, Z., Balasenthil, S., Nguyen, D., Sahin, A.A., den Hollander, P., and Kumar, R. (2004). Dynein light chain 1, a p21-activated kinase 1-interacting substrate, promotes cancerous phenotypes. Cancer Cell *5*, 575–585.
8. Kumar, R., Sanawar, R., Li, X., and Li, F. (2017). Structure, biochemistry, and biology of PAK kinases. Gene *605*, 20–31.
9. Mazumdar, A., and Kumar, R. (2003). Estrogen regulation of Pak1 and FKHR pathways in breast cancer cells. FEBS Lett. *535*, 6–10.
10. Xu, J., Liu, H., Chen, L., Wang, S., Zhou, L., Yun, X., Sun, L., Wen, Y., and Gu, J. (2012). Hepatitis B virus X protein confers resistance of hepatoma cells to anoikis by up-regulating and activating p21-activated kinase 1. Gastroenterology *143*, 199–212.
11. Halaban, R. (2015). RAC1 and melanoma. Clin. Ther. *37*, 682–685.
12. Li, X., Liu, F., and Li, F. (2010). PAK as a therapeutic target in gastric cancer. Expert Opin. Ther. Targets *14*, 419–433.
13. Wu, W.K., Lee, C.W., Cho, C.H., Fan, D., Wu, K., Yu, J., and Sung, J.J. (2010). MicroRNA dysregulation in gastric cancer: a new player enters the game. Oncogene *29*, 5761–5771.
14. Jerraya, H., Saidani, A., Khalfallah, M., Bouasker, I., Nouira, R., and Dziri, C. (2013). Management of liver metastases from gastric carcinoma: where is the evidence? Tunis. Med. *91*, 1–5.
15. Go, P.H., Klaassen, Z., Meadows, M.C., and Chamberlain, R.S. (2011). Gastrointestinal cancer and brain metastasis: a rare and ominous sign. Cancer *117*, 3630–3640.
16. Bartel, D.P. (2009). MicroRNAs: target recognition and regulatory functions. Cell *136*, 215–233.
17. Shi, Z., Wei, Q., and She, J. (2014). MicroRNAs in gastric cancer metastasis. Crit. Rev. Eukaryot. Gene Expr. *24*, 39–53.
18. Cheng, Z., Liu, F., Wang, G., Li, Y., Zhang, H., and Li, F. (2014). miR-133 is a key negative regulator of CDC42-PAK pathway in gastric cancer. Cell. Signal. *26*, 2667–2673.
19. Reddy, S.D., Ohshiro, K., Rayala, S.K., and Kumar, R. (2008). MicroRNA-7, a homeobox D10 target, inhibits p21-activated kinase 1 and regulates its functions. Cancer Res. *68*, 8195–8200.
20. Parrini, M.C., Lei, M., Harrison, S.C., and Mayer, B.J. (2002). Pak1 kinase homodimers are autoinhibited in trans and dissociated upon activation by Cdc42 and Rac1. Mol. Cell *9*, 73–83.
21. Magill, S.T., Cambronne, X.A., Luikart, B.W., Lioy, D.T., Leighton, B.H., Westbrook, G.L., Mandel, G., and Goodman, R.H. (2010). microRNA-132 regulates dendritic growth and arborization of newborn neurons in the adult hippocampus. Proc. Natl. Acad. Sci. USA *107*, 20382–20387.
22. Ching, Y.P., Leong, V.Y., Lee, M.F., Xu, H.T., Jin, D.Y., and Ng, I.O. (2007). P21-activated protein kinase is overexpressed in hepatocellular carcinoma and enhances cancer metastasis involving c-Jun NH2-terminal kinase activation and paxillin phosphorylation. Cancer Res. *67*, 3601–3608.
23. Zarubin, T., and Han, J. (2005). Activation and signaling of the p38 MAP kinase pathway. Cell Res. *15*, 11–18.
24. Gozdecka, M., and Breitwieser, W. (2012). The roles of ATF2 (activating transcription factor 2) in tumorigenesis. Biochem. Soc. Trans. *40*, 230–234.
25. Yasuda, M., Tanaka, Y., Fujii, K., and Yasumoto, K. (2001). CD44 stimulation downregulates Fas expression and Fas-mediated apoptosis of lung cancer cells. Int. Immunol. *13*, 1309–1319.
26. Salmon, H., Franciszkiewicz, K., Damotte, D., Dieu-Nosjean, M.C., Validire, P., Trautmann, A., Mami-Chouaib, F., and Donnadieu, E. (2012). Matrix architecture

defines the preferential localization and migration of T cells into the stroma of human lung tumors. J. Clin. Invest. *122*, 899–910.

27. Kou, B., Gao, Y., Du, C., Shi, Q., Xu, S., Wang, C.Q., Wang, X., He, D., and Guo, P. (2014). miR-145 inhibits invasion of bladder cancer cells by targeting PAK1. Urol. Oncol. *32*, 846–854.
28. Zhang, X., Mao, H., Chen, J.Y., Wen, S., Li, D., Ye, M., and Lv, Z. (2013). Increased expression of microRNA-221 inhibits PAK1 in endothelial progenitor cells and impairs its function via c-Raf/MEK/ERK pathway. Biochem. Biophys. Res. Commun. *431*, 404–408.
29. Claps, G., Cheli, Y., Zhang, T., Scortegagna, M., Lau, E., Kim, H., Qi, J., Li, J.L., James, B., Dzung, A., et al. (2016). A transcriptionally inactive ATF2 variant drives melanomagenesis. Cell Rep. *15*, 1884–1892.
30. Vlahopoulos, S.A., Logotheti, S., Mikas, D., Giarika, A., Gorgoulis, V., and Zoumpourlis, V. (2008). The role of ATF-2 in oncogenesis. BioEssays *30*, 314–327.
31. Sevilla, A., Santos, C.R., Vega, F.M., and Lazo, P.A. (2004). Human vaccinia-related kinase 1 (VRK1) activates the ATF2 transcriptional activity by novel phosphorylation on Thr-73 and Ser-62 and cooperates with JNK. J. Biol. Chem. *279*, 27458–27465.
32. Bhoumik, A., and Ronai, Z. (2008). ATF2: a transcription factor that elicits oncogenic or tumor suppressor activities. Cell Cycle *7*, 2341–2345.
33. Harper, K.L., Sosa, M.S., Entenberg, D., Hosseini, H., Cheung, J.F., Nobre, R., Avivar-Valderas, A., Nagi, C., Girnius, N., Davis, R.J., et al. (2016). Mechanism of early dissemination and metastasis in Her2+ mammary cancer. Nature, Published online December 14, 2016. http://dx.doi.org/10.1038/nature20609.
34. Jacobs, P.P., and Sackstein, R. (2011). CD44 and HCELL: preventing hematogenous metastasis at step 1. FEBS Lett. *585*, 3148–3158.
35. Orian-Rousseau, V. (2010). CD44, a therapeutic target for metastasising tumours. Eur. J. Cancer *46*, 1271–1277.
36. Van Obberghen-Schilling, E., Tucker, R.P., Saupe, F., Gasser, I., Cseh, B., and Orend, G. (2011). Fibronectin and tenascin-C: accomplices in vascular morphogenesis during development and tumor growth. Int. J. Dev. Biol. *55*, 511–525.
37. Zhang, L., Huang, D., Wang, Q., Shen, D., Wang, Y., Chen, B., Zhang, J., and Gai, L. (2014). MiR-132 inhibits expression of SIRT1 and induces pro-inflammatory processes of vascular endothelial inflammation through blockade of the SREBP-1c metabolic pathway. Cardiovasc. Drugs Ther. *28*, 303–311.
38. Cheng, F., Su, L., Yao, C., Liu, L., Shen, J., Liu, C., Chen, X., Luo, Y., Jiang, L., Shan, J., et al. (2016). SIRT1 promotes epithelial-mesenchymal transition and metastasis in colorectal cancer by regulating Fra-1 expression. Cancer Lett. *375*, 274–283.
39. Xiang, L., Ren, Y., Cai, H., Zhao, W., and Song, Y. (2015). MicroRNA-132 aggravates epileptiform discharges via suppression of BDNF/TrkB signaling in cultured hippocampal neurons. Brain Res. *1622*, 484–495.
40. Tili, E., Michaille, J.J., and Croce, C.M. (2013). MicroRNAs play a central role in molecular dysfunctions linking inflammation with cancer. Immunol. Rev. *253*, 167–184.
41. Chou, J., Shahi, P., and Werb, Z. (2013). microRNA-mediated regulation of the tumor microenvironment. Cell Cycle *12*, 3262–3271.
42. Jasinski-Bergner, S., Mandelboim, O., and Seliger, B. (2014). The role of microRNAs in the control of innate immune response in cancer. J. Natl. Cancer Inst. *106*, dju257.
43. Ueda, R., Kohanbash, G., Sasaki, K., Fujita, M., Zhu, X., Kastenhuber, E.R., McDonald, H.A., Potter, D.M., Hamilton, R.L., Lotze, M.T., et al. (2009). Dicer-regulated microRNAs 222 and 339 promote resistance of cancer cells to cytotoxic T-lymphocytes by down-regulation of ICAM-1. Proc. Natl. Acad. Sci. USA *106*, 10746–10751.
44. O'Neill, L.A. (2009). Boosting the brain's ability to block inflammation via microRNA-132. Immunity *31*, 854–855.
45. Wanet, A., Tacheny, A., Arnould, T., and Renard, P. (2012). miR-212/132 expression and functions: within and beyond the neuronal compartment. Nucleic Acids Res. *40*, 4742–4753.
46. Zhang, Z.G., Chen, W.X., Wu, Y.H., Liang, H.F., and Zhang, B.X. (2014). MiR-132 prohibits proliferation, invasion, migration, and metastasis in breast cancer by targeting HN1. Biochem. Biophys. Res. Commun. *454*, 109–114.
47. Zhang, B., Lu, L., Zhang, X., Ye, W., Wu, J., Xi, Q., and Zhang, X. (2014). Hsa-miR-132 regulates apoptosis in non-small cell lung cancer independent of acetylcholinesterase. J. Mol. Neurosci. *53*, 335–344.
48. Wang, J., Xu, G., Shen, F., and Kang, Y. (2014). miR-132 targeting cyclin E1 suppresses cell proliferation in osteosarcoma cells. Tumour Biol. *35*, 4859–4865.
49. Formosa, A., Lena, A.M., Markert, E.K., Cortelli, S., Miano, R., Mauriello, A., Croce, N., Vandesompele, J., Mestdagh, P., Finazzi-Agrò, E., et al. (2013). DNA methylation silences miR-132 in prostate cancer. Oncogene *32*, 127–134.
50. Park, J.K., Henry, J.C., Jiang, J., Esau, C., Gusev, Y., Lerner, M.R., Postier, R.G., Brackett, D.J., and Schmittgen, T.D. (2011). miR-132 and miR-212 are increased in pancreatic cancer and target the retinoblastoma tumor suppressor. Biochem. Biophys. Res. Commun. *406*, 518–523.
51. Nakamura, K., Tomioku, M., Nabeshima, K., and Yasuda, S. (2014). Clinicopathologic features and clinical outcomes of gastric cancer patients with bone metastasis. Tokai J. Exp. Clin. Med. *39*, 193–198.
52. Liu, T., Li, Y., Gu, H., Zhu, G., Li, J., Cao, L., and Li, F. (2013). p21-Activated kinase 6 (PAK6) inhibits prostate cancer growth via phosphorylation of androgen receptor and tumorigenic E3 ligase murine double minute-2 (Mdm2). J. Biol. Chem. *288*, 3359–3369.
53. Zhang, J., Wang, J., Guo, Q., Wang, Y., Zhou, Y., Peng, H., Cheng, M., Zhao, D., and Li, F. (2012). LCH-7749944, a novel and potent p21-activated kinase 4 inhibitor, suppresses proliferation and invasion in human gastric cancer cells. Cancer Lett. *317*, 24–32.
54. Abba, M., Benner, A., Patil, N., Heil, O., and Allgayer, H. (2015). Differentially expressed microRNAs in colorectal cancer metastasis. Genom. Data *6*, 33–35.